Rock and Soil Mechanics

Volume 44 | Issue 7 Article 5

11-3-2023

A simplified algorithm for predicting creep settlement of high fill based on modified power law model

Jian HUANG
School of Civil and Transportation Engineering, Beijing University of Civil Engineering and Architecture, Beijing 100044, China, huangjian@bucea.edu.cn

Pu-rong DE
School of Civil and Transportation Engineering, Beijing University of Civil Engineering and Architecture, Beijing 100044, China

Yang-ping YAO
School of Transportation Science and Engineering, Beihang University, Beijing 100191, China

Ren PENG
Beijing Municipal Construction Co., Ltd., Beijing 100045, China

See next page for additional authors

A simplified algorithm for predicting creep settlement of high fill based on modified power law model

Abstract

The creep settlement dominates the long-term deformation of high fill foundation after construction and cannot be ignored. The reliable prediction of creep settlement provides an important guideline for judging whether settlement is stable and arranging subsequent construction. The modification of the traditional power law model for predicting the one-dimensional creep deformation of soil is proposed, which can describe the one dimensional creep deformation of clay, sand and soil-rock mixture. The modified model satisfies the requirement that the growth of the creep deformation has an asymptote with respect to time; that is to say, the creep deformation grows continually and approaches a constant with time. The proposed model has only two parameters, which can be easily obtained from oedometer tests. Then, a simplified algorithm to predict the creep settlement of high fill foundation is developed based on the proposed model. The simplified algorithm has two parameters, which can be determined using the field settlement monitoring data. Based on the field settlement monitoring data of high fill in Longnan Chengxian Airport, Cangyuan Washan Airport and Lüliang Dawu Airport, the fitting and prediction results of the proposed simplified algorithm are compared with those of other three curve fitting algorithms commonly used in geotechnical engineering. The results show that the proposed simplified algorithm can predict the creep settlement of high fill foundation more effectively and accurately.

Keywords

high fill, foundation, creep settlement, settlement prediction

Authors

Jian HUANG, Pu-rong DE, Yang-ping YAO, Ren PENG, and Ji-lin QI

Rock and Soil Mechanics 2023 44(7): 2095−2104 ISSN 1000−7598
https: //doi.org/10.16285/j.rsm.2022.6245 http://rocksoilmech.researchcommons.org/journal

A simplified algorithm for predicting creep settlement of high fill based on modified power law model

HUANG Jian[1], DE Pu-rong[1], YAO Yang-ping[2], PENG Ren[3], QI Ji-lin[1]

1. School of Civil and Transportation Engineering, Beijing University of Civil Engineering and Architecture, Beijing 100044, China
2. School of Transportation Science and Engineering, Beihang University, Beijing 100191, China
3. Beijing Municipal Construction Co., Ltd., Beijing 100045, China

Abstract: The creep settlement dominates the long-term deformation of high fill foundation after construction and cannot be ignored. The reliable prediction of creep settlement provides an important guideline for judging whether settlement is stable and arranging subsequent construction. The modification of the traditional power law model for predicting the one-dimensional creep deformation of soil is proposed, which can describe the one-dimensional creep deformation of clay, sand and soil-rock mixture. The modified model satisfies the requirement that the growth of the creep deformation has an asymptote with respect to time; that is to say, the creep deformation grows continually and approaches a constant with time. The proposed model has only two parameters, which can be easily obtained from oedometer tests. Then, a simplified algorithm to predict the creep settlement of high fill foundation is developed based on the proposed model. The simplified algorithm has two parameters, which can be determined using the field settlement monitoring data. Based on the field settlement monitoring data of high fill in Longnan Chengxian Airport, Cangyuan Washan Airport and Lüliang Dawu Airport, the fitting and prediction results of the proposed simplified algorithm are compared with those of other three curve fitting algorithms commonly used in geotechnical engineering. The results show that the proposed simplified algorithm can predict the creep settlement of high fill foundation more effectively and accurately.

Keywords: high fill; foundation; creep settlement; settlement prediction

1 Introduction

With China's economic development, the construction of transportation infrastructures such as airports, high-speed railways and expressways have been extended to the mountainous areas with vast areas and gullies, which results in lots of high-fill foundations[1]. The large volume and high height of the fill lead to the long-term creep settlement of the fill and the original ground under a high self-gravitational stress[2−4]. Airport runways, railway tracks and expressways cannot be paved until the settlement of the fill reaches a stable state. Otherwise, excessive settlement or uneven settlement could seriously threaten the safe operation of those roads. It is necessary to monitor when the settlement of high fill foundations reaches a stable value, and to calculate and predict the variation trend of the creep settlement based on the monitoring data.

There are four main prediction methods for the creep settlement: (i) the layerwise summation method recommended by standards[5], (ii) the curve-fitting method[6], (iii) the numerical modelling method represented by finite element method[7], and (iv) the system analysis method represented by artificial neural networks[8]. Among them, the curve fitting method is to propose a time-dependent model to predict the variation trend of creep settlement, and to optimize the model parameters through the in-situ settlement monitoring results, and then to predict the long-term creep settlement. The curve-fitting method is concise and practical, therefore it is widely used in practical engineering. Various commonly-used functions have been developed, such as a logarithmic function[9], a power function[10], a hyperbolic function[11], and a exponential function[12]. The logarithmic function and the power function are dispersive, which increase slowly with time and do not stop completely. Namely, the settlement tends to an infinite value when the t approaches $+\infty$, which is not consistent with the reality[13−14]. The hyperbolic function and the exponential function may underestimate the creep settlement, and the growth curve as the exponential function is prone to overfitting[6].

The fill material of high fill is generally the soil-rock mixture obtained in the excavation area, so the creep settlement of the high fill is determined by the creep behavior of the soil and the rock together. The creep curve of soil is generally described by the classical semi-logarithmic curve. Numerous experimental studies have indicated that the power law model rather than the semi-log law may be consistent with the creep behavior of coarse-grained materials[15−20]. Briaud and Garland[10], Briaud and Gibben[21], and Bi et al.[22] have shown that the power

Received: 9 August 2022 Accepted: 7 November 2022
This work was supported by the National Natural Science Foundation of China (52108293), Beijing Postdoctoral Research Foundation of China (2021-zz-106) and the Fundamental Research Funds for Beijing University of Civil Engineering and Architecture (X21072).
First author: HUANG Jian, male, born in 1988, PhD, Reader, research interests: geotechnical engineering. E-mail: huangjian@bucea.edu.cn
Corresponding author: QI Ji-lin, male, born in 1969, PhD, Professor, PhD supervisor, research interests: frozen soil mechanics and engineering in cold regions. E-mail: jilinqi@bucea.edu.cn

law model can give a good prediction for the one-dimensional compression and the creep deformation in a triaxial condition of the clay and the fine sand with silt. However, the power law model is not satisfactory in describing the long-term creep tendency. The power law model needs to be further modified to better describe the creep behavior of the soil-rock mixture in a unified way, which can be used for predicting the creep settlement of the high fill.

In this paper, the traditional power law model was modified, and a new creep deformation formula was developed. The reliability of the proposed creep deformation formula was verified by the consolidation tests on the clay and the clay-sand mixture and the previous one-dimensional creep test results on the soil-rock mixture. Then, a simplified algorithm for predicting the creep settlement was developed based on the formula. Finally, the feasibility of the simplified algorithm was justified by using the settlement monitoring results at three high fills, such as the Longnan Chengxian Airport. The prediction results by the three other curve-fitting methods commonly used in geotechnical engineering were compared with the simplified algorithm, which indicated that the proposed algorithm gave reliable and accurate prediction results.

2 Background

2.1 Modified power law-based creep deformation model

The deformation of a soil element in consolidation tests consists of instantaneous deformation, primary consolidation and secondary consolidation (or creep deformation). It is assumed that those three deformations are completely independent, and that the instantaneous deformation and the primary consolidation are elasto-plastic deformation. Thus, only creep deformation develops in the soil element after the completion of primary consolidation. The creep deformation versus time, t starts at the end of the primary consolidation. The symbol, T stands for the period which starts from the beginning of consolidation test loading.

Briaud and garland[10] proposed a power law model to describe the rate of loading effect when driving a pile in the clay. Briaud and Gibbens[21], Bi et al.[22] further extended the power law model to describe the creep deformation of sand and clay in one-dimensional compression and triaxial compression with a low or medium confining stress, which can be expressed by the following equation:

$$\frac{\varepsilon_{\mathrm{t}}}{\varepsilon_1}=\left(\frac{t}{t_1}\right)^n \tag{1}$$

where ε_{t} is the creep deformation at a time t since the beginning of the loading; ε_1 is the deformation value for a reference time t_1 which can be arbitrary (e.g., 1 s, 1 min, or 1 d); and n is the viscous exponent of the soil.

Equation (1) indicates that the relationship between the deformation and the time can be represented by a straight line with the slope of n on the log−log plot $\lg(\varepsilon/\varepsilon_1)$−$\lg(t/t_1)$. The test results of clay and fine sand with silt demonstrate that Eq. (1) gives reliable estimation of the creep deformation for a certain time if only creep deformation occurs[21−22]. However, the creep deformation increases with increasing time t and finally tends to infinite. The study has shown that the creep deformation of the soil-rock mixtures under one-dimensional compression and drained triaxial compression with a low or medium confining stress level eventually leaves off at a constant value[13]; that is to say, the creep deformation curve should have a horizontal asymptote parallel to the time axis. Therefore, the power law model can be modified based on Eq. (1):

$$\frac{\varepsilon_{\mathrm{t}\infty}-\varepsilon_{\mathrm{t}}}{\varepsilon_{\mathrm{t}\infty}}=\left(\frac{t}{t_0}+1\right)^{-n} \tag{2}$$

where $\varepsilon_{\mathrm{t}\infty}$ is the creep deformation at the creep time t approaching infinite; t_0 is the unit time used as normalizing creep time.

Thus, Eq. (3) gives the expression for creep deformation ε_{t} based on Eq. (2):

$$\varepsilon_{\mathrm{t}}=\varepsilon_{\mathrm{t}\infty}-\varepsilon_{\mathrm{t}\infty}\left(\frac{t}{t_0}+1\right)^{-n} \tag{3}$$

Equation (3) indicates that $\varepsilon_{\mathrm{t}}=0$ when $t=0$ and $\varepsilon_{\mathrm{t}}=\varepsilon_{\mathrm{t}\infty}$ when t approaches $+\infty$. The creep deformation increases nonlinearly with time to a stable value $\varepsilon_{\mathrm{t}\infty}$. Compared with Eq. (1), Eq. (3) is more realistic for predicting the soil creep deformation.

Based on the assumption that the elasto-plastic deformation consists of the instantaneous deformation and the primary consolidation, the total soil deformation can be expressed as:

$$\varepsilon=\varepsilon_{\mathrm{t}}+\varepsilon_{\mathrm{ep}} \tag{4}$$

where ε is the total deformation since the beginning of the consolidation test; and $\varepsilon_{\mathrm{ep}}$ is the elasto-plastic deformation.

Similarly, the difference between the total deformation ε_∞ and the creep deformation $\varepsilon_{\mathrm{t}\infty}$ when the creep time t approaches $+\infty$ is $\varepsilon_{\mathrm{ep}}$, i.e.

$$\varepsilon_\infty=\varepsilon_{\mathrm{t}\infty}+\varepsilon_{\mathrm{ep}} \tag{5}$$

where ε_∞ is the total deformation when the soil deformation reaches the steady state in consolidation tests.

Equations (3) and (5) gives

$$\varepsilon_{\mathrm{t}}=\left(\varepsilon_\infty-\varepsilon_{\mathrm{ep}}\right)\left[1-\left(\frac{t}{t_0}+1\right)^{-n}\right] \tag{6}$$

Equation (6) indicates that $\varepsilon_{\mathrm{t}}=0$ at $t=0$ and $\varepsilon_{\mathrm{t}}=\varepsilon_{\mathrm{t}\infty}=\varepsilon_\infty-\varepsilon_{\mathrm{ep}}$ when the creep time t approaches infinite.

https://rocksoilmech.researchcommons.org/journal/vol44/iss7/5
DOI: 10.16285/j.rsm.2022.6245

Equations (4) and (6) gives

$$\varepsilon = \varepsilon_\infty - \left(\varepsilon_\infty - \varepsilon_{ep}\right)\left(\frac{t}{t_0}+1\right)^{-n} \tag{7}$$

Equation (7) indicates that $\varepsilon = \varepsilon_{ep}$ at $t = 0$; namely, the soil deformation at the beginning of creep only consists of the instantaneous deformation and the primary consolidation. When the creep time t approaches infinite, $\varepsilon = \varepsilon_\infty$, i.e., the soil deformation increases nonlinearly with time and reaches the stable value of ε_∞.

2.2 Model validation

2.2.1 Validation method and determination of model parameters

Based on Eq. (2), it can be found that the relationship between the creep deformation and the time can be represented by a straight line with the slope of $-n$ on the log−log plot $\lg[(\varepsilon_{t\infty}-\varepsilon_t)/\varepsilon_{t\infty}]-\lg(t/t_0+1)$. As the total soil deformation in the consolidation test contains the instantaneous deformation, the primary consolidation, and the creep deformation, Eq. (2) can be rewritten as the expression with ε. Substituting Eqs. (4) and (5) into Eq. (2) yields

$$\frac{\varepsilon_\infty - \varepsilon}{\varepsilon_{t\infty}} = \left(\frac{t}{t_0}+1\right)^{-n} \tag{8}$$

Multiplying both hand sides of Eq. (8) simultaneously by $\varepsilon_{t\infty}/\varepsilon_\infty$ gives

$$\frac{\varepsilon_\infty - \varepsilon}{\varepsilon_\infty} = \frac{\varepsilon_{t\infty}}{\varepsilon_\infty}\left(\frac{t}{t_0}+1\right)^{-n} \tag{9}$$

Taking a logarithm on both hand sides of Eq. (9) and combining with Eq. (5) gives

$$\lg\left(\frac{\varepsilon_\infty - \varepsilon}{\varepsilon_\infty}\right) = \lg\left(\frac{\varepsilon_\infty - \varepsilon_{ep}}{\varepsilon_\infty}\right) - n\lg\left(\frac{t}{t_0}+1\right) \tag{10}$$

Equation (10) indicates that the relationship between the deformation and the time obtained from consolidation tests can be represented by a straight line with the slope of $-n$ on the log−log plot. For the clay, ε_{ep} is the soil deformation corresponding to the transit point between the primary and the secondary consolidations, which can be determined on the ε–lg$t$ plot. For the soil-rock mixture, the elasto-plastic deformation and the creep deformation are generally bounded by one hour; namely, the instantaneous soil deformation takes place during the first hour since the beginning of the loading[16–17]. The ε_∞ can be determined by the following two methods: (i) Conduct the one-dimensional creep test on a given soil with different over-consolidation ratios, then find the location of the stable deformation through the relationship between the creep deformation and the over-consolidation ratio, and finally solve ε_∞ under a given load[12]. (ii) Take ε_∞ in Eq. (7) as the model parameter to determine ε_∞ inversely by a optimization algorithm based on the deformation versus time results of one-dimensional creep tests. The first method requires multiple tests, so the second method is used to determine ε_∞ in the present study.

2.2.2 Consolidation tests on clay and sand

The consolidation tests were carried out on a clay and a clay-sand mixture. Then, the test results were used to validate the modified power law model. The clay used in this study was obtained from a construction site in Xiamen, Fujian, China. The sand used in this study was the Chinese ISO standard sand produced by Xiamen ISO Standard Sand Co., Ltd. The sand was a medium sand with the grain size ranging from 0.5 mm to 1.0 mm. The clay and the clay-sand mixture were used for the consolidation tests. The clay-sand mixture was prepared by mixing the clay and the Chinese ISO standard sand in the ratio of 2∶3 by weight. Three identical specimens were prepared for the clay and the clay-sand mixture, each of which were used for consolidation tests with three different final load steps of 200, 400 and 800 kPa. After air-drying, the specific gravity, liquid limit and plastic limit of the clay and the clay-sand mixture were measured. The air-dried soil was placed in the consolidation test device and consolidated under the vertical load of 25 kPa. The basic physical properties of the two soils were determined in accordance with *Standard for geotechnical test method* (GB/T 50123−2019)[23], as shown in Table 1. Because the grain size of the Chinese ISO standard sand does not meet the requirement of the limit water content tests, i.e., the grain size should be less than 0.5 mm, the liquid limit, plastic limit and plasticity index of the clay-sand mixture were not included in Table 1. According to the standard GB/T 50123−2019, the consolidation tests were conducted on two soils with four load steps, i.e., 100 kPa, 200 kPa, 400 kPa, and 800 kPa. Three identical specimens of each soil were loaded step by step with the final load of 200 kPa, 400 kPa, and 800 kPa, respectively. Dial readings were recorded for each load step in accordance with the standard GB/T 50123−2019, and the duration from the beginning of the final load to the end of the test was eight days.

Table 1 Basic physical properties of clay and clay-sand mixture

Soil	Dry density /(g • cm^{-3})	Specific gravity	Initial void ratio	Liquid limit /%	Plastic limit /%	Plasticity index
Clay	1.39	2.75	0.964	30.71	15.61	15.1
Clay-sand mixture	1.62	2.70	0.668	—	—	—

Figures 1 and 2 show the ε versus lg$T$ curves for the

clay and the clay-sand mixture under different vertical loads.

The primary consolidation and the secondary consolidation for the clay and the clay-sand mixture specimens under different final loads were extracted and replotted using the same time axis, as shown in Figs. 3 and 4.

As shown in Figs. 3 and 4, the secondary consolidation in the ε–lg$T$ curves for both the clay and the clay-sand mixture under different final loads are linear on the semi-log plot and the slopes are approximately the same. It indicates that the creep deformation of normally consolidated soils at a regular stress level is independent of stress levels. As shown in Table 2, the parameters ε_{ep}, ε_{∞}, and n in Eq. (10) were determined from the consolidation test results on the clay and the clay-sand mixture under different final loads. Thus, the test results were shown on a log−log plot according to Eq. (10), as shown in Figs. 5 and 6.

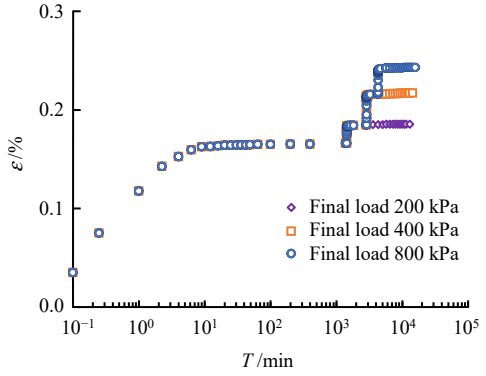

Fig. 1 The ε–T curves of clay under different loads

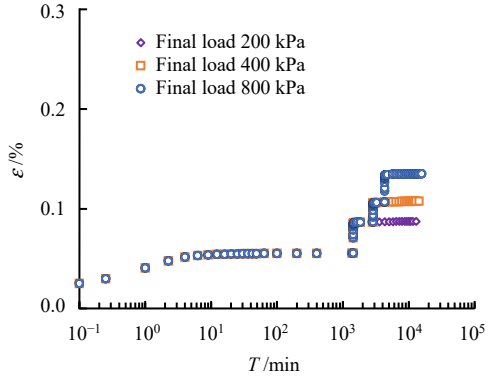

Fig. 2 The ε–T curves of clay-sand mixture under different loads

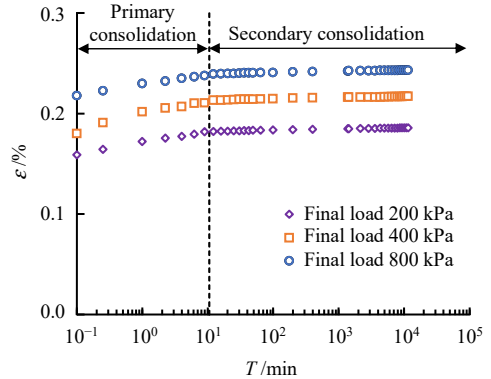

Fig. 3 The ε–T curves of clay under different loads

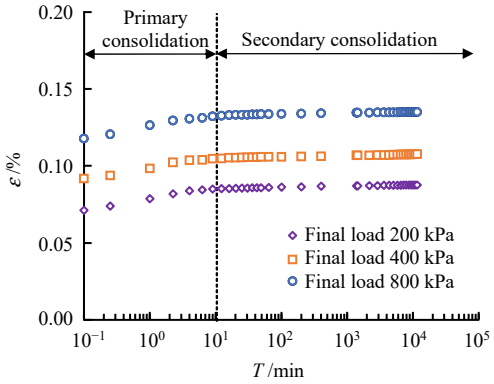

Fig. 4 The ε–T curves of clay-sand mixture under different loads

Table 2 Creep model parameters of clay and clay-sand mixture

Load /kPa	Clay			Clay-sand mixture		
	ε_{ep} /%	ε_{∞} /%	n	ε_{ep} /%	ε_{∞} /%	n
200	0.181	0.196	0.038	0.085	0.515	0.064
400	0.212	0.228	0.039	0.105	0.484	0.071
800	0.239	0.254	0.039	0.132	0.439	0.065

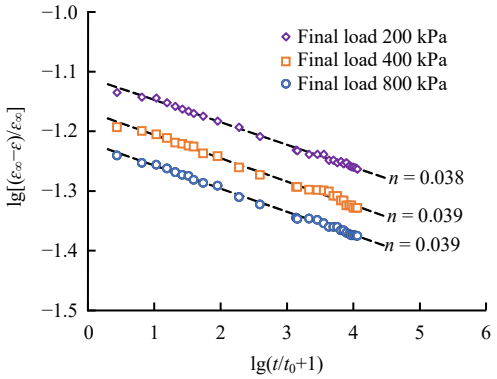

Fig. 5 The lg[(ε_{∞}−ε)/ε_{∞}]−lg(t/t_0+1) curves of clay under different loads

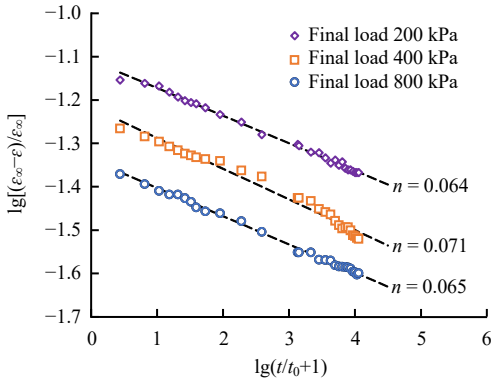

Fig. 6 The lg[(ε_{∞}−ε)/ε_{∞}]−lg(t/t_0+1) curves of clay-sand mixture under different loads

As shown in Figs. 5 and 6, the relationship between deformation and time of the clay and the clay-sand mixture under different final loads are linear on the log−log plot, i.e., lg[(ε_{∞}−ε)/ε_{∞}]−lg(t/t_0+1), and the slopes are approximately the same. It indicates that Eq. (10) derived from the modified power law model is consistent with the consolidation

behavior of the clay and the clay-sand mixture. Since Eq. (10) is derived from Eq. (6), Eq. (6) can give a good estimation of the creep deformation of the clay and the clay-sand mixture.

2.2.3 One-dimensional creep tests of soil-rock mixture

Zhang et al.[24] carried out one-dimensional creep tests using a large consolidation apparatus on the scaled soil-rock mixture taken from the left bank of Hongshiyan landslide dam in Niulan River in Yunnan, China. The initial load was 50 kPa, and the subsequent load increment was equal to the previous load. The subsequent load was applied until the settlement of the specimen was stable, i.e., not greater than 0.05 mm per hour. The creep test results for different final loads of 0.8 MPa, 1.6 MPa, and 3.2 MPa are presented on a ε–lg$t$ plot, as shown in Fig. 7.

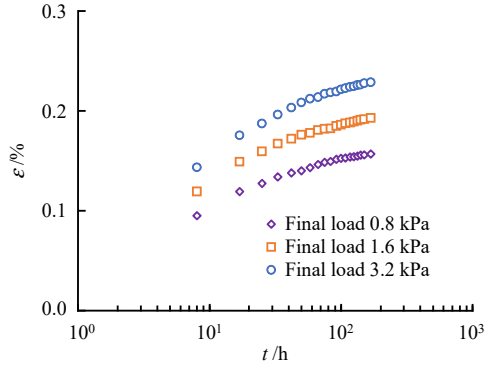

Fig. 7 The ε–t curves of soil-rock mixture under different loads

As shown in Fig. 7, the settlement versus time curves of the soil-rock mixture under different loads are nonlinear on the ε–lg$t$ plot. The linear relationship on the semi-log plot cannot represent the creep behavior of the crushed rock materials, which is consist of the previous experimental studies[15−20]. As shown in Table 3, the parameters ε_{ep}, ε_{∞}, and n in Eq. (10) were determined from the consolidation test results on the soil-rock mixture under different final loads. Thus, the test results were shown on a log−log plot according to Eq. (10), as shown in Fig. 8.

Table 3 Creep model parameters of soil-rock mixture

Load /MPa	ε_{ep} /%	ε_{∞} /%	n
0.8	0.095	0.199	0.276
1.6	0.120	0.239	0.280
3.2	0.144	0.278	0.299

As shown in Fig. 8, the relationship between deformation and time of the soil-rock mixture under different final loads are linear on the log−log plot, i.e., lg[(ε_{∞}−ε)/ε_{∞}]−lg(t/t_0+1), and the slopes are approximately the same. It indicates that Eq. (10) derived from the modified power law model is consistent with the consolidation behavior of the soil-rock mixture. Thus, Eq. (6) can give a good estimation of the creep deformation of the soil-rock mixture.

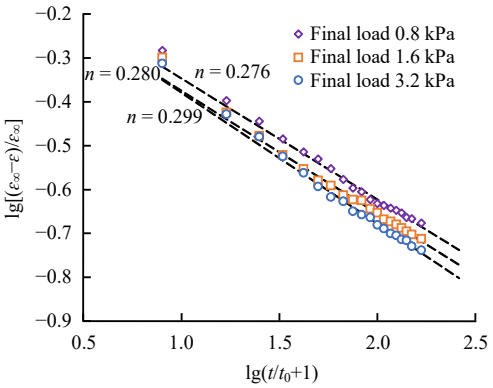

Fig. 8 The lg[(ε_{∞}−ε)/ε_{∞}]−lg(t/t_0+1) curves of soil-rock mixture under different loads

In summary, Eq. (6) can be used to estimate the creep deformation of clays, clay-sand mixtures, and soil-rock mixtures. Thus, Eq. (6) can also be used for predicting the creep settlement of the high fill with soil-rock mixtures.

3 Simplified algorithm for predicting creep settlement of high fill

3.1 Simplified algorithm

When using the layerwise summation method to estimate the creep settlement of high fill foundations, the settlement of soil layer i at creep time t can be obtained from Eq. (6):

$$\hat{s}_i = \varepsilon_{ti} H_i = \left(\varepsilon_{\infty i} - \varepsilon_{epi}\right) H_i \left[1 - \left(\frac{t}{t_0} + 1\right)^{-n_i}\right] \tag{11}$$

where H_i is the thickness of the soil layer i; ε_{epi}, $\varepsilon_{\infty i}$ and n_i are the deformation at the beginning of creep, the deformation at the moment the creep stabilizes, and the viscosity exponent of the soil layer i, which can be determined by consolidation test results; and ε_{ti} is the creep deformation at a time t of the soil layer i.

Equation (11) indicates that the creep settlement of the high fill depends exclusively on time once the model parameters of each soil layer are determined. Thus, the creep settlement s of the high fill at the creep time t is

$$s = \sum_{i=1}^{m} \hat{s}_i = \sum_{i=1}^{m} \left(\varepsilon_{\infty i} - \varepsilon_{epi}\right) H_i \left[1 - \left(\frac{t}{t_0} + 1\right)^{-n_i}\right] \tag{12}$$

where m is the total number of soil layers in the high fill.

The model parameters of each soil layer are required to estimate the creep settlement of the high fill by the layerwise summation method, i.e., Eq. (12). Typically, it is difficult to obtain those model parameters due to the complicated construction environment and tight project schedule. Therefore, a simplified method is needed for

predicting the creep settlement of the high-fill when the model parameters of each soil layer are incomplete and the in-situ settlement monitoring data is limited. Due to a large filling area, the stress state in the high fill can be approximated as one-dimensional compression[6, 25]. Therefore, the estimation method for the one-dimensional creep deformation of soil can be extended to predict the creep settlement of the high-fill. When the high-fill body and the original ground are regarded as a whole, a simplified algorithm is proposed to predict the creep settlement s based on Eq. (6):

$$\frac{s}{s_0}=\alpha\left[1-\left(\frac{t}{t_0}+1\right)^{-\beta}\right] \tag{13}$$

where s_0 is the unit settlement used as normalizing creep settlement s; and α and β are model parameters.

3.2 Determination of model parameters

The parameters α and β in Eq. (13) can be determined by inversion analysis of the monitoring data of creep settlement. The specific steps include (i) to adopt the minimum value of the sum of squares of the errors between the creep settlement monitoring values and the predicted values as the objective function f, i.e., Eq. (14); (ii) to use optimization algorithms such as the genetic algorithm to automatically search the optimal parameters.

$$\left.\begin{aligned} f&=\min\sum_{j=1}^{p}\left(s_j-\hat{s}_j\right)^2\\ \hat{s}_j&=\alpha\left[1-\left(\frac{t_j}{t_0}+1\right)^{-\beta}\right]s_0\end{aligned}\right\} \tag{14}$$

where p is the number of settlement monitoring; t_j is the moment for the j^{th} monitoring; s_j is the j^{th} in-situ monitoring value; and $\hat{s}_j$ is the estimated creep settlement at the creep time is t_j.

4 Case studies and algorithm comparison

4.1 Comparative studies with other three models

To verify the reliability of the proposed algorithm for predicting the creep settlement on the basis of limited measured data, the other three widely used methods were selected for comparative studies. The Hoshino method is proposed based on the Terzaghi consolidation theory[26]. It is also found that the settlement is proportional to the square root of time based on the field settlement monitoring results, which can be written as

$$s=s_0'+\frac{\alpha\beta\sqrt{t-t_0'}}{\sqrt{1+\beta^2\left(t-t_0'\right)}} \tag{15}$$

where t_0' and s_0' are the time and the corresponding settlement at the starting reference point for settlement calculation, respectively. Generally, $t_0'=0$ and $s_0'=0$.

The hyperbolic model was proposed by Sridharan et al.[11], who assumed a simplified hyperbolic relationship between the settlement and time:

$$s=s_0'+\frac{t-t_0'}{\alpha+\beta\left(t-t_0'\right)} \tag{16}$$

Richards model is a growth curve method, which is highly compatible and can degenerate to other settlement predictive models with specific model parameter values of γ. For example, when $\gamma=0$, Richards model becomes the three-point method; when $\gamma=2$, Richards model becomes the Logistic model; when $\gamma\geqslant 1$ and assuming that $n=\gamma-1$, Richards model becomes Usher model. Therefore, Richards model is also commonly used for predicting the creep settlement of ground[12], which can be expressed by

$$s=s_\infty\left(1-\alpha\mathrm{e}^{-\beta t}\right)^{\frac{1}{1-\gamma}} \tag{17}$$

where s_∞ is a model parameter and equivalent to the final settlement.

The coefficient of determination, R^2 is chosen as the evaluation index for the different prediction models or algorithms[27]. The value of R^2 ranges from $-\infty$ to 1. The closer to unity is R^2, the better curve-fitting result the predictive model has. The formula of R^2 is

$$R^2=1-\frac{\sum_{j=1}^{p}\left(s_j-\hat{s}_j\right)^2}{\sum_{j=1}^{p}\left(s_j-\overline{s}\right)^2} \tag{18}$$

where $\overline{s}$ is the average value of the settlement monitoring results. The model parameters of each model were determined through the curve-fitting section of the monitoring data. With the determined model parameters, the predictive settlement by different models were plotted. Finally, the curve-fitting and prediction by different models can be evaluated using Eq. (18) to calculate the value of R^2 with the estimated values and field monitoring data for curve-fitting and prediction sections.

4.2 Creep settlement prediction of Longnan Chengxian Airport

Longnan Chengxian Airport located in Longnan, Gansu Province, China, is a high-fill airport with the maximum slope height of 60 m and constructed with the soil-rock mixtures from the excavated area. The airport reached the design elevation of the test section in early January 2015. The design elevation was later changed, and the fill height was increased by 84 cm in early January 2016, when the field settlement monitoring started[28]. Based on the settlement monitoring data at points DM3 and DM4 of Longnan Chengxian Airport, the settlement prediction

results by Hoshino model, hyperbolic model, Richards model and the simplified algorithm proposed in present study were compared. The specific steps included: (i) assume that only the monitoring data for the first 172 d was known, and the model parameters of the four models were determined using the known monitoring data from 0 to 172 d; (ii) calculate the correlation coefficients for four models during the period from 0 to 172 d to justify the feasibility of the model parameters; and (iii) compare the long-term settlement prediction using the four models with monitoring results for 352 d. The model parameters of each algorithm determined from the monitoring data during the first 172 d at monitoring points DM3 and DM4 are shown in Tables 4 and 5. The R^2 values for the curve-fitting and prediction stages, and the stable values of settlement (i.e., ultimate settlement value or settlement value when the settlement rate is not greater than 0.02 mm /d, which has the same meaning hereinafter) are also shown in Tables 4 and 5. Figs. 9 and 10 show the comparison between the predictions using different models based on the fitting parameters in Tables 4 and 5 with settlement measurements at points DM3 and DM4, respectively.

Table 4 Algorithm parameters obtained based on 172 d field settlement monitoring data of point DM3 in Longnan Chengxian Airport

Method	Model parameters	R^2		Stable settlement value /mm
		Curve-fitting	Prediction	
Hoshino method	$\alpha=269.952$, $\beta=0.004$	0.931	−0.849	269.94
Hyperbolic model	$\alpha=7.913$, $\beta=0.020$	0.977	0.619	51.05
Richards model	$s_\infty=18.158$, $\alpha=0.940$, $\beta=0.013$, $\gamma=0.477$	0.982	−1.671	18.16
Simplified algorithm	$\alpha=-0.254$, $\beta=-0.801$	0.973	0.898	705.12

Table 5 Algorithm parameters obtained based on 172 d field settlement monitoring data of point DM4 in Longnan Chengxian Airport

Method	Model parameters	R^2		Stable settlement value /mm
		Curve-fitting	Prediction	
Hoshino method	$\alpha=1\,063.835$, $\beta=0.003$	0.949	−1.146	1 063.77
Hyperbolic model	$\alpha=3.040$, $\beta=0.004$	0.978	0.912	222.27
Richards model	$s_\infty=56.412$, $\alpha=1.132$, $\beta=0.012$, $\gamma=0.407$	0.991	−0.887	56.41
Simplified algorithm	$\alpha=-0.527$, $\beta=-0.860$	0.981	0.957	2 058.51

As shown in Figs. 9 and 10, the monitored settlements fluctuated in the first 172 d, which are used for model parameters determination. The Hoshino model has a poor fitting result, while the other three algorithms fit well with the monitoring data for the first 172 d. The Richards model has four model parameters and its curve shape can vary flexibly, the curve-fitting results show an overfitting phenomenon. For predicting the creep settlement from 172 to 352 d, the proposed simplified algorithm shows a remarkably better performance than the other three methods.

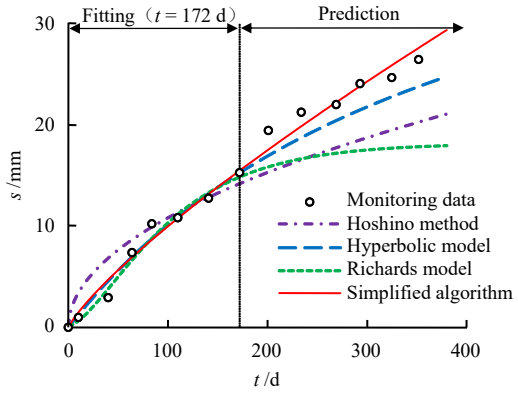

Fig. 9 Comparison of prediction curves of different algorithms for point DM3 in Longnan Chengxian Airport

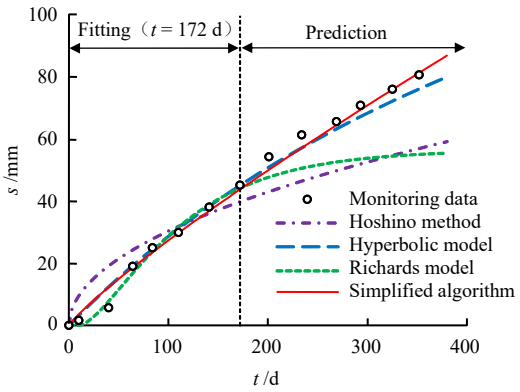

Fig. 10 Comparison of prediction curves of different algorithms for point DM4 in Longnan Chengxian Airport

4.3 Creep settlement prediction of Cangyuan Washan Airport

Cangyuan Washan Airport located in Lincang, Yunnan Province, China, is a typical high-fill airport. The maximum height of the fill is over 98 m, and the fill material is mainly the soil-rock mixture from the excavated area. The in-situ settlement monitoring started on July 11, 2015, after the high fill was completed. Based on the settlement monitoring data at monitoring points C21 and C23 at Cangyuan Washan Airport, the prediction accuracy of the proposed simplified algorithm and the other three models were compared[29]. The model parameters of each prediction algorithm were determined using the monitoring data for the first 80 d. Then, the corresponding prediction curves with the determined parameters were plotted, which were compared with the monitoring data at each monitoring point from 80 d to 196 d. The model parameters, the R^2

values for the fitting and prediction stages, and the stable values of settlement at monitoring points C21 and C23 are shown in Tables 6 and 7. Figs. 11 and 12 show the prediction curves of four different algorithms based on the model parameters in Tables 6 and 7.

Table 6 Algorithm parameters obtained based on 80 d field settlement monitoring data of point C21 in Cangyuan Washan Airport

Method	Model parameters	R^2		Final settlement value /mm
		Curve-fitting	Prediction	
Hoshino method	$\alpha=299.384$, $\beta=0.025$	0.991	0.380	299.36
Hyperbolic model	$\alpha=0.393$, $\beta=0.010$	0.998	0.495	96.31
Richards model	$s_\infty=87.085$, $\alpha=1.028$, $\beta=0.013$, $\gamma=-0.653$	0.999	0.746	87.08
Simplified algorithm	$\alpha=-20.052$, $\beta=-0.328$	0.993	0.920	283.63

Table 7 Algorithm parameters obtained based on 80 d field settlement monitoring data at point C23 in Cangyuan Washan Airport

Method	Model parameters	R^2		Final settlement value /mm
		Curve-fitting	Prediction	
Hoshino method	$\alpha=1071.431$, $\beta=0.008$	0.991	−0.336	629.21
Hyperbolic model	$\alpha=0.380$, $\beta=0.009$	0.996	0.427	109.26
Richards model	$s_\infty=86.285$, $\alpha=1.023$, $\beta=0.019$, $\gamma=-0.330$	0.998	−0.338	86.28
Simplified algorithm	$\alpha=-22.455$, $\beta=-0.324$	0.993	0.911	321.65

As shown in Figs. 11 and 12, the prediction curves using each algorithm fit well with the monitoring data for the first 80 d. On the other hand, the proposed simplified algorithm has a remarkably better prediction performance than the other three algorithms, when predicting the monitored creep settlements from 80 d to 196 d.

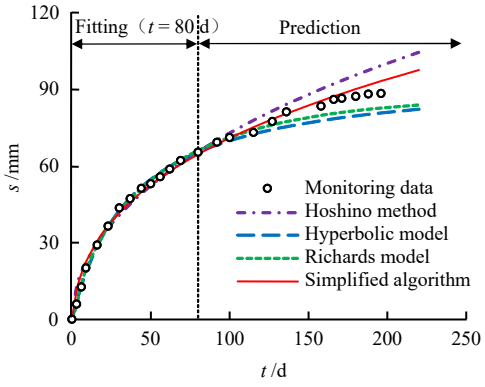

Fig. 11 Comparison of prediction curves of different algorithms for point C21 in Cangyuan Washan Airport

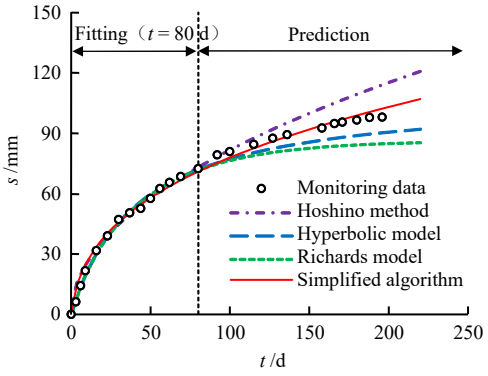

Fig. 12 Comparison of prediction curves of different algorithms for point C23 in Cangyuan Washan Airport

4.4 Creep settlement prediction of Lüliang Dawu Airport

Lüliang Dawu Airport is located in Lüliang, Shanxi Province, China. The high fill has a maximum height of 85 m and the fill material is mainly excavated loess. The in-situ settlement monitoring data provided the settlement at monitoring points 0-3 and 0-4 in the fill area for 343 d since the fill was completed[30]. The model parameters of each prediction algorithm were determined using the monitoring data for the first 153 d. Then, the corresponding prediction curves with the determined parameters were plotted, which were compared with the monitoring data at each monitoring point from 153 d to 343 d. The model parameters, the R^2 values for the fitting and prediction stages, and the stable values of settlement at monitoring points 0-3 and 0-4 are shown in Tables 8 and 9. Figs. 13 and 14 show the prediction curves of four different algorithms based on the model parameters in Tables 8 and 9.

As shown in Figs. 13 and 14, the prediction curves using each algorithm fit well with the monitoring data for the first 153 d. On the other hand, the proposed simplified algorithm gives better and more stable predictions than the other three algorithms, when predicting the monitored creep settlements from 153 d to 343 d.

Table 8 Algorithm parameters obtained based on 153 d field settlement monitoring data of point 0-3 in Lüliang Dawu Airport

Method	Model parameters	R^2		Final settlement value /mm
		Curve-fitting	Prediction	
Hoshino method	$\alpha=3\,457.020$, $\beta=0.005$	0.985	0.963	3 456.94
Hyperbolic model	$\alpha=0.323$, $\beta=0.003$	0.996	0.764	368.50
Richards model	$s_\infty=274.026$, $\alpha=1.064$, $\beta=0.008$, $\gamma=-0.408$	0.999	0.516	274.03
Simplified algorithm	$\alpha=-17.690$, $\beta=-0.503$	0.994	0.981	5 821.83

Table 9 Algorithm parameters obtained based on 153 d field settlement monitoring data of point 0-4 in Lüliang Dawu Airport

Method	Model parameters	R^2		Final settlement value /mm
		Curve-fitting	Prediction	
Hoshino method	$\alpha=3\ 172.798$, $\beta=0.004$	0.993	0.247	2 458.40
Hyperbolic model	$\alpha=0.397$, $\beta=0.004$	0.999	0.829	237.93
Richards model	$s_\infty=327.038$, $\alpha=1.018$, $\beta=0.002$, $\gamma=-1.024$	0.999	0.835	327.04
Simplified algorithm	$\alpha=-18.809$, $\beta=-0.431$	0.997	0.796	1 511.01

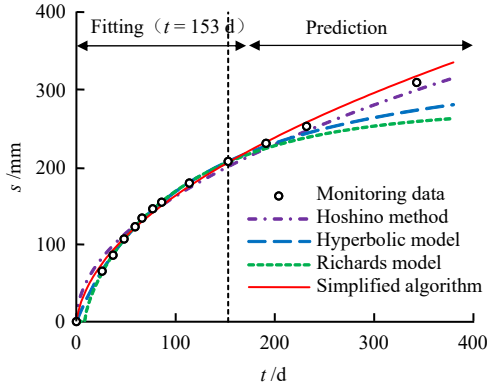

Fig. 13 Comparison of prediction curves of different algorithms for point 0-3 in Lüliang Dawu Airport

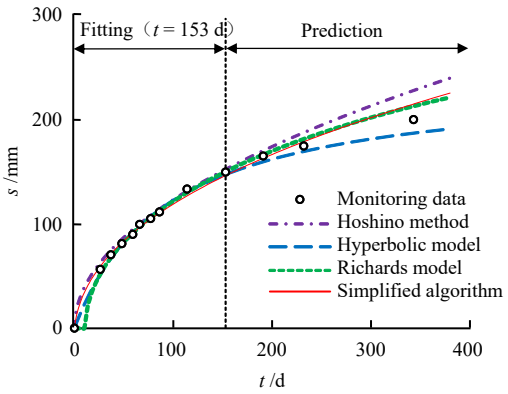

Fig. 14 Comparison of prediction curves of different algorithms for point 0-4 in Lüliang Dawu Airport

The coefficients of determination listed in Tables 4 to 9 indicate that the R^2 values for the prediction of each algorithm are significantly smaller than those for the curve-fitting. The prediction accuracy decreases with time. Therefore, if the prediction of settlement is based on part of monitoring data, the prediction is more accurate when the moment is closer to the range of monitoring period for determining the model parameters. It can be inferred that an effective prediction interval exists in the condition of a given error limit[31].

5 Conclusions

In this paper, based on the modified power law model, the creep deformation formula was derived which can describe the one-dimensional creep behavior of clays, sands, and soil-rock mixtures. In addition, a simplified algorithm for estimating the creep settlement of the high-fill ground is proposed. The main conclusions are summarized as follows:

(1) Due to the limitations of the conventional power law model, a modified power law model was developed for predicting the creep deformation. The proposed one-dimensional creep deformation formula based on the modified power law model can describe the creep deformation behavior of clays, sands, and soil-rock mixtures. The proposed formula meets the requirement that the creep deformation increases nonlinearly with time and finally reaches a stable value. In addition, all the model parameters can be determined by the consolidation test.

(2) A simplified algorithm for creep deformation of high-fill grounds was developed based on the derived one-dimensional creep deformation formula. The algorithm has only two parameters and can be determined by inversion of the settlement monitoring data.

(3) The feasibility of the proposed simplified algorithm was examined by the settlement monitoring data of high-fill grounds at three different airports. Comparison between the prediction results using the simplified algorithm and those by other three models commonly used in geotechnical engineering indicates that the proposed simplified algorithm can predict the creep settlement of high fills more effectively and accurately.

(4) The proposed simplified algorithm provides an effective tool for estimating and predicting the creep settlement of high-fill grounds. However, the applicability of the simplified algorithm to special soils such as expansive soils, collapsible loess and frozen soils needs further studies.

References

[1] YANG Zhou, CHENG Xiao-hui, MA Qiang, et al. Study of strength indices for undrained stability analysis of high filled ground[J]. Rock and Soil Mechanics, 2022, 43(1): 218−226.

[2] YAO Yang-ping, HUANG Jian, ZHANG Kui, et al. Numerical back-analysis of creep settlement of airport high fill[J]. Rock and Soil Mechanics, 2020, 41(10): 3395−3404, 3414.

[3] YAO Yang-ping, LIU Lin, WANG Lin, et al. Method of calculating creep deformation of high filled embankment[J]. Rock and Soil Mechanics, 2015, 36(Suppl.1): 154−158.

[4] YAO Yang-ping, WANG Jun-bo. Application of Beidou satellite positioning to deformation remote monitoring of high fill airport[J]. Rock and Soil Mechanics, 2018, 39(Suppl.1): 419−424.

[5] Civil Aviation Administration of China. MH/T5027−2013

Code for geotechnical engineering design of airport[S]. Beijing: China Civil Aviation Publishing House, 2013.

[6] YAO Y P, HUANG J, WANG N D, et al. Prediction method of creep settlement considering abrupt factors[J]. Transportation Geotechnics, 2020, 22: 100304.

[7] ZHU Cai-hui, LI Ning. Post-construction settlement analysis of loess-high filling based on time-dependent deformation experiments[J]. Rock and Soil Mechanics, 2015, 36(10): 3023−3031.

[8] KANAYAMA M, ROHE A, PAASSEN L V. Using and improving neural network models for ground settlement prediction[J]. Geotechnical and Geological Engineering, 2014, 32(3): 687−697.

[9] YAO Yang-ping, QI Sheng-jun, CHE Li-wen. Computational method of post-construction settlement for high-fill embankments[J]. Journal of Hydroelectric Engineering, 2016, 35(3): 1−10.

[10] BRIAUD J L, GARLAND E. Loading rate method for pile response in clay[J]. Journal of Geotechnical Engineering, 1985, 111(3): 319−335.

[11] SRIDHARAN A, MURTHY N S, PRAKASH K. Rectangular hyperbola method of consolidation analysis[J]. Géotechnique, 1987, 37(3): 355−368.

[12] HUANG C F, LI Q, WU S C, et al. Application of the Richards model for settlement prediction based on a bidirectional difference-weighted least-squares method[J]. Arabian Journal for Science and Engineering, 2018, 43(10): 5057−5065.

[13] YAO Y P, FANG Y F. Negative creep of soils[J]. Canadian Geotechnical Journal, 2019, 57(1): 1−16.

[14] FENG W Q, LALIT B, YIN Z Y, et al. Long-term non-linear creep and swelling behavior of Hong Kong marine deposits in oedometer condition[J]. Computers and Geotechnics, 2017, 84: 1−15.

[15] KUWANO R, JARDINE R J. On measuring creep behaviour in granular materials through triaxial testing[J]. Canadian Geotechnical Journal, 2002, 39(5): 1061−1074.

[16] CHENG Zhan-lin, DING Hong-shun. Creep test for rockfill[J]. Chinese Journal of Geotechnical Engineering, 2004, 26(4): 473−476.

[17] CHENG Zhan-lin, DING Hong-shun. Experimental study on engineering characteristics of rockfill materials[J]. Yangtze River, 2007, 38(7): 110−114, 120.

[18] LI Hai-fang, ZHANG Qin-cheng, XU Ze-ping, et al. Test study on creep characteristics of dam foundation rockfill of Xilongchi lower reservoir[J]. Chinese Journal of Rock Mechanics and Engineering, 2009, 28(Suppl.2): 3376−3382.

[19] LI Hai-fang, ZHANG Yin-qi, JIN Wei, et al. Experimental study on rockfill creep modeling[J]. Journal of Hydroelectric Engineering, 2013, 32(1): 212−217.

[20] SUN Geng, ZHANG Yin-qi, LI Hai-fang. The research of rockfill creep model and parameters[J]. Journal of China Institute of Water Resources and Hydropower Research, 2016, 14(2): 115−121.

[21] BRIAUD J L, GIBBENS R. Behavior of five large spread footings in sand[J]. Journal of Geotechnical and Geoenvironmental Engineering, 1999, 125(9): 787−796.

[22] BI G, BRIAUD J L, SANCHEZ M, et al. Power law model to predict creep movement and creep failure[J]. Journal of Geotechnical and Geoenvironmental Engineering, 2019, 145(9): 04019044.

[23] Ministry of Housing and Urban-Rural Development of the People's Republic of China, State Administration for Market Regulation. GB/T50123−2019 Standard for geotechnical testing method[S]. Beijing: China Planning Press, 2019.

[24] ZHANG Yan-yi, DENG Gang, WEN Yan-feng, et al. Experimental study on consolidation-rheology characteristics of soil-aggregate mixture materials[J]. Journal of Hydroelectric Engineering, 2021, 40(2): 187−194.

[25] CAO Guang-xu, SONG Er-xiang, XU Ming. Study on experiment and calculation method of dry-wet cycle characteristics of rockfills[J]. Journal of Harbin Institute of Technology, 2011, 43(10): 98−104.

[26] Jiangsu Expressway Company Limited, Hohai University. Engineering manual for soft clay subgrade of communication construction[M]. Beijing: Publishing Company of People's Communication, 2001.

[27] MEI Shi-ang, CHEN Sheng-shui, ZHONG Qi-ming, et al. Parametric model for breaching analysis of earth-rock dam[J]. Advanced Engineering Sciences, 2018, 50(2): 60−66.

[28] YANG Xiao-hui, ZHU Yan-peng, ZHOU Yong, et al. Time-space monitoring and stability analysis of high fill slope slip process at a airport in mountain region[J]. Chinese Journal of Rock Mechanics and Engineering, 2016, 35(Suppl.2): 3977−3990.

[29] YANG Shao-shuai. Research of rainfall effect on the high fill foundation of a Yunnan airport[D]. Chengdu: Chengdu University of Technology, 2017.

[30] ZHU Cai-hui, LI Ning, LIU Ming-zhen, et al. Spatiotemporal laws of post-construction settlement of loess-filled foundation of Lüliang airport[J]. Chinese Journal of Geotechnical Engineering, 2013, 35(2): 293−301.

[31] YAO Yang-ping, WANG Shen, WANG Nai-dong, et al. Prediction method for long-term settlements of high-speed railway subgrade under influences of nearby loads[J]. Chinese Journal of Geotechnical Engineering, 2019, 41(4): 625−630.